



Effect of boron incorporation on the lattice parameter and texture of diamond films deposited by chemical vapour deposition on silicon

D. Chateigner^{a,*}, F. Brunet^a, A. Deneuveille^b, P. Germi^a, M. Pernet^a,
E. Gheeraert^b, P. Gonon^b

^a *Laboratoire de Cristallographie, CNRS, BP166, F-38042 Grenoble Cedex 09, France*

^b *Laboratoire d'Etude des Propriétés Electroniques des Solides, CNRS, BP166, F-38042 Grenoble Cedex 09, France*

Received 22 September 1994; manuscript received in final form 25 November 1994

Abstract

Incorporation of boron in polycrystalline diamond films deposited on Si is shown to decrease or increase the lattice parameter below and above about 10^{19} B cm⁻³, respectively. At lower values of doping, the lattice parameter is lower than that of the undoped films, while their $\langle 111 \rangle$ texture is maintained. At higher values, the lattice parameter increases rapidly above that of the undoped films, while the $\langle 111 \rangle$ texture is progressively lost until it becomes untextured at 6×10^{20} B cm⁻³. A coherent interpretation of these results is proposed, based on a decrease and an increase of the defect concentration with B incorporation below and above 10^{19} B cm⁻³, with the hypothesis that the defects increase the diamond lattice parameter.

1. Introduction

Diamond has various excellent physical properties which might be used now when its preparation as thin films has been achieved. Its wide bandgap, high electron and hole mobilities, and high thermal conductivity are well suited for high temperature electronics which, on the other hand, need basically monocrystalline films, control of the resistivity by the doping and control of space charge zone extent by applied voltage.

The restricted area of natural and synthetic diamond crystals at this moment pushes one to

look for heteroepitaxy ideally on well-known materials. Limited heteroepitaxial growth on substrates offering good lattice matching with diamond, as cubic-BN or Ni, has been reported [1]. Silicon has a very large lattice mismatch (52%) with diamond. Mainly $\langle 220 \rangle$, sometimes $\langle 100 \rangle$ and once $\langle 111 \rangle$ textures [2–5], have been reported for polycrystalline diamond films on silicon. However, in spite of their large mismatch, a negative bias voltage applied to the substrate has been reported to allow very high orientation (10° of misorientation of the crystallite basal planes with regard to the in-plane substrate orientation) of undoped diamond on (001) β -SiC [6,8] or Si [7,8], if the growing conditions for $\langle 001 \rangle$ texturation are kept [8].

* Corresponding author.

Incorporation of boron into diamond films is needed to achieve devices, but it might change the deposition mechanism (therefore, the growth mechanism) in the chemical vapour deposition (CVD) processes, for instance above the concentration corresponding to a sudden decrease in its deposition rate [9].

In this paper, the effect of boron incorporation on the texture and the lattice parameters of 1.5 and 10 μm thick polycrystalline diamond films deposited on (100) and (111) single-crystal silicon substrates is studied.

2. Experimental details

The diamond films are deposited by microwave plasma assisted chemical vapour deposition (MPCVD) on silicon substrates at 730 and 880°C from a gas mixture containing 99.5% H_2 /0.5% CH_4 and 200 to 10 000 ppm of B_2H_6 with a total gas flow of 100 SCCM and a total pressure of 30 Torr. The substrate holder is in silica (to avoid metallic incorporation) and stands in the middle of the plasma ball. The thicknesses of the films were determined from the spacing of the interference fringes obtained by infrared transmission. The boron concentration in the film was measured by secondary ion mass spectroscopy (SIMS) and calibrated on undoped films implanted with known boron doses.

Among the different possibilities for X-ray texture analyses (θ - 2θ peak ratios, rocking curves, φ -scans), the pole figure technique using the Schulz reflection method [10] has been used, because it is particularly efficient and offers a more precise and detailed macroscopic characterization. The X-ray texture analysis was made with a Courbon S.A. texture sample holder mounted on a horizontal θ - 2θ GMI goniometer. The Cu $\text{K}\alpha$ radiation was supplied by a Rigaku RU300E rotating anode which allows a maximum power of 60 kV \times 300 mA. The incident beam is monochromatized by the (002) reflection of a flat graphite specimen of 0.4° mosaic spread, which is essential for the study of thin films deposited on single crystalline substrates [11]. The beam is collimated by two crossed slits and the diffracted

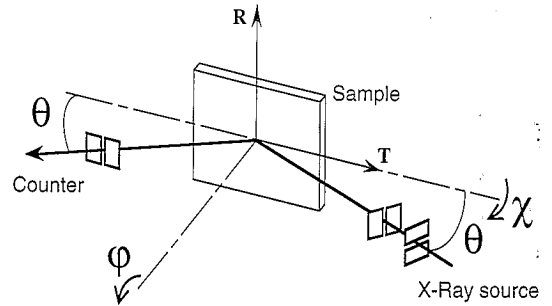


Fig. 1. Schematic representation of the Schulz texture analysis method in the reflection geometry. Note that scans of the tilt (χ) and azimuthal (φ) angles do not change the Bragg angle value for one pole figure (one $\{hkl\}$ plane family).

line is detected through a horizontal slit by a proportional counter. The signal is filtered by an SCA tension switcher and the data are finally corrected for background and peak defocusing [12], assuming a linear absorption coefficient of X-ray radiation in diamond equal to 16.17 cm^{-1} . The pole figure layout is realized with a Compaq 486/50 computer fed by our own programs (Cortexg, Phiscan and Pofint). In the Schulz method (Fig. 1), the sample is rotated around a tilt angle χ , and an azimuthal angle φ , which both keep constant the Bragg angle θ , i.e. one $\{hkl\}$ plane family. Therefore, each measured intensity $I(\chi, \varphi)$ is proportional to the number of $\{hkl\}$ lattice planes that are in diffraction position in each sample orientation (χ, φ).

Diamond films deposited by MPCVD have been reported to exhibit preferred orientations in the $\langle 110 \rangle$ [2–5], $\langle 100 \rangle$ [4,5] and $\langle 111 \rangle$ [5] directions. Our samples exhibited (400) X-ray reflection, so weak in θ - 2θ scans that they were supposed to have no $\langle 100 \rangle$ preferred orientation. Therefore, the texture of the films was analysed through the $\langle 111 \rangle$ and $\langle 220 \rangle$ pole figures.

3. Results and interpretation

3.1. Boron concentration in the solid phase

Seven 1.5 μm thick samples and three 10 μm thick samples of various boron content were deposited at 730 and 880°C on (100) and (111)

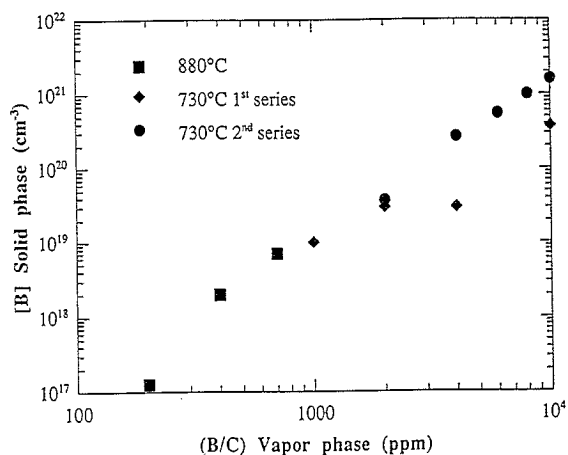


Fig. 2. Variation of the effective boron concentration $[B]$ versus the imposed boron gas ratio in the reaction chamber. Under these experimental conditions this concentration saturates near 10^{21} cm^{-3} .

oriented Si substrates, respectively. The amount of boron incorporated in the film ($[B]$, expressed in atoms/ cm^3) depends on the relative concentration of boron to carbon in the vapour phase ($2\text{B}_2\text{H}_6/\text{CH}_4$ in ppm). Fig. 2 shows the variation of the boron concentration $[B]$ in the solid phase versus that in the gas phase between 200 and 10 000 ppm. There is a monotonic increase from $[B] = 10^{17} \text{ cm}^{-3}$ at 200 ppm to $[B] = 1.62 \times 10^{21} \text{ cm}^{-3}$ at 10 000 ppm.

3.2. Lattice parameter of diamond

Both the (111) and the (220) interplanar distances were measured to check deformation of

the unit cell. Classical θ - 2θ scans by 0.01° steps were done around the Bragg angle positions of (111) and (220) reflections. Due to the different focusing geometry, optimized here for pole figure measurements, peaks are broader than measured with a classical powder diffractometer. Therefore, the barycenter of each peak was taken as the mean angular position. Both the (111) and the (220) interplanar distances increase with the boron content in our concentration range, more rapidly above about $10^{19} \text{ B cm}^{-3}$ (Figs. 3a and 3b). They are lower than those of undoped films in the range 10^{17} to about $10^{20} \text{ B cm}^{-3}$ and higher above about $10^{20} \text{ B cm}^{-3}$, respectively, with a total relative variation of about 5×10^{-3} between 10^{17} and $1.62 \times 10^{21} \text{ B cm}^{-3}$. Within the experimental uncertainty, the lattice remains cubic.

3.3. Texture of boron doped films

From the knowledge of the shifted Bragg angle values, the texture of five $1.5 \mu\text{m}$ thick samples deposited at 730°C on Si(100) was examined. From previous work [13], the $\langle 111 \rangle$ fiber texture is favoured for undoped films at this deposition temperature. The $\{111\}$ pole figures of our samples having the lower ($3.75 \times 10^{19} \text{ cm}^{-3}$) and the higher ($1.62 \times 10^{21} \text{ cm}^{-3}$) B incorporation level are shown in Fig. 4. The $\langle 111 \rangle$ fiber-like texture is completely kept when $[B] = 3.75 \times 10^{19} \text{ cm}^{-3}$ (Fig. 4a), while at our higher values of $[B] = 1.62 \times 10^{21} \text{ cm}^{-3}$ (Fig. 4b), it is completely lost, the

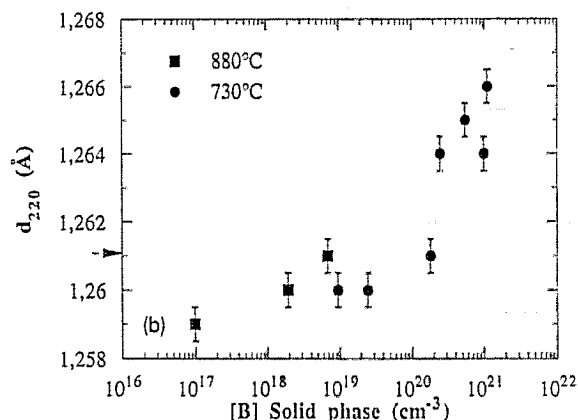
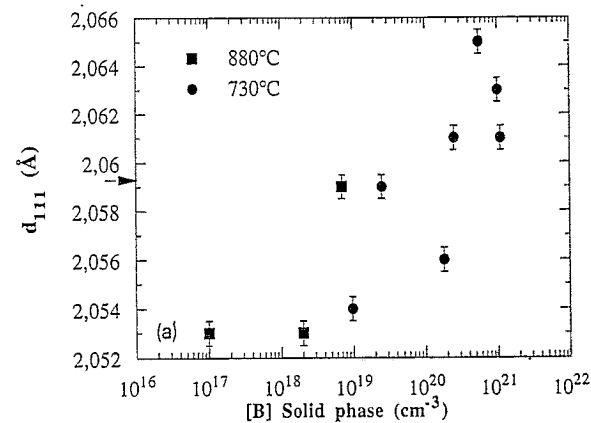


Fig. 3. Evolution with $[B]$ of (a) the d_{111} and (b) the d_{220} interatomic distances of doped diamond. The values corresponding to undoped diamond are indicated by arrows.

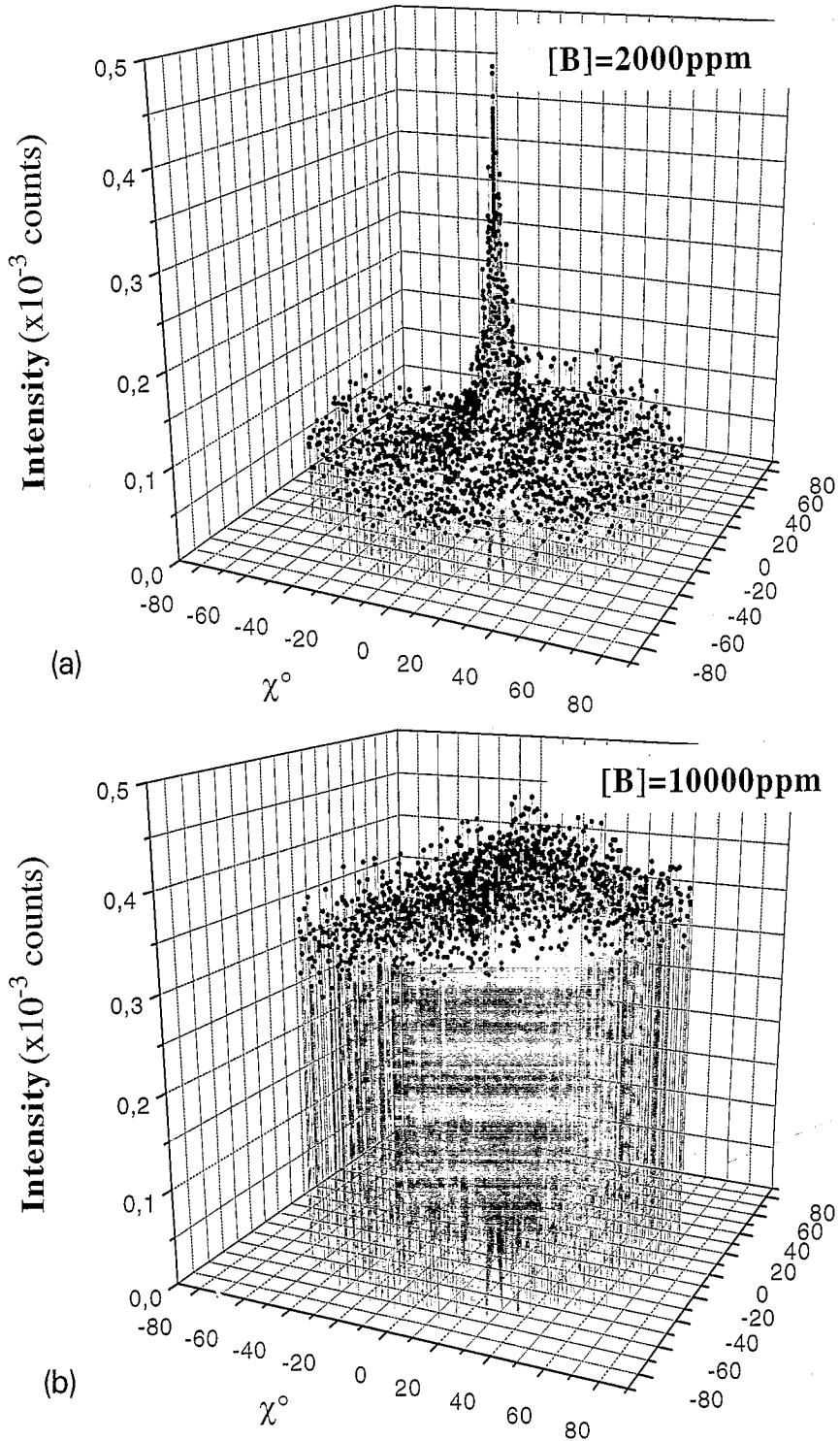


Fig. 4. {111} pole figures of 1.5 μm thick B-doped diamond films deposited at 730°C on (100) oriented Si with [B] = 2.5 × 10¹⁹ atoms/cm³ (a) and [B] = 1.1 × 10²² atoms/cm³ (b).

films exhibiting on the contrary a quite random distribution of the crystallites. Actually, this randomness was observed as soon as $[B] = 6 \times 10^{20} \text{ cm}^{-3}$.

4. Discussion

4.1. Lattice parameters of boron-doped diamond films

The isotropic expansion of the cubic cell in this range of B incorporation agrees with the other published studies [14–16]. While Ran et al. [14] report a lattice parameter independent of the B content, according to both Voronov and Rakhmanina [15] and Spitsyn et al. [16] it increases with [B], as found here. However, the reported parameters according to [B] compared with those of the undoped samples (quite similar here and in Refs. [15,16]) are quite different: Voronov and Rakhmanina [15] report a continuous increase from the value of the undoped samples with a total relative variation up to 3×10^{-3} at $1.76 \times 10^{21} \text{ cm}^{-3}$, while Spitsyn et al. [16] report an increase with [B] up to the value of the undoped diamond, which is reached when $[B] = 1.76 \times 10^{21} \text{ cm}^{-3}$. Our results are in between. They agree with the parameters corresponding to the lower and higher incorporation level of Spitsyn et al. [16] and Voronov and Rakhmanina [15], respectively, and with the latter authors for the beginning of significant lattice expansion above about $10^{19} \text{ B cm}^{-3}$. The origin of the variation of the lattice parameter with B incorporation is not clear. According to Spitsyn et al. [16], contraction of the lattice results from B incorporation on substitutional (doping) sites, while expansion results from B in interstitial (defective) sites, and Voronov and Rakhmanina [15] suggest that expansion begins at the [B] transition from semiconductor to metallic state. From the variations of the full width at half maximum of the Raman peaks, we already suggested [9] interaction between defects and doping level improving the quality of the film up to about $B/C = 1000 \text{ ppm}$ ($[B] = 10^{19} \text{ cm}^{-3}$), and formation of an impurity band (and hopping conduction) from direct inter-

action between the B atoms [17]. This interpretation can also explain the present results, and agrees with some previous suggestions [15,16]: incorporation of B atoms on substitutional (doping) sites at low level decreases the concentration of defects, and therefore contracts the lattice if we suppose that the defects are expanding the lattice. The interaction between (substitutional) B atoms (when the impurity band appears) induces the formation of defects which expand the lattice parameter. Quite generally, the diamond lattice parameter seems highly sensitive to incorporation of foreign atoms [15,16] (which interact with crystallographic defects). Therefore, their interaction (or that of crystallographic defects) with B might explain the differences in the value of the lattice parameter with the same [B] when different impurities from different preparation processes are used (microwave plasma assisted chemical vapour deposition here, high pressure and temperature [15], and chemical transport reaction [16]).

4.2. Texture of boron-doped diamond films

There is no report, to our knowledge, on the effect of B incorporation, while there are several studies [2–5] on the relationship between the texture and the preparation conditions of thick ($> 15 \mu\text{m}$) undoped polycrystalline diamond films on Si. Their interpretations [2–5] are based on the evolutionary model [17]. From this model, Wild et al. [4c] predict admixture of $\langle 100 \rangle$ and $\langle 110 \rangle$ texture for a deposition temperature of 730°C and $0.5\% \text{CH}_4/99.5\% \text{H}_2$, while we find systematically (which excludes the “odd” sample) $\langle 111 \rangle$ textures for undoped as well as B incorporation $< 6 \times 10^{20} \text{ cm}^{-3}$. These differences might originate from those in the preparation processes. In particular, we do not use an external substrate heater, and therefore, the substrate temperature and the supply in hydrocarbon radicals are not independent under our preparation conditions. While the $\langle 111 \rangle$ texture of the undoped films is kept up to $3.75 \times 10^{19} \text{ B cm}^{-3}$, it is progressively lost up to randomness, with higher B incorporation up to $6 \times 10^{20} \text{ cm}^{-3}$. After the completion of an impurity band (around $[B] = 10^{19} \text{ B cm}^{-3}$),

this corresponds to an increasing interaction between B atoms shifting the conduction process from hopping conduction to metallic conductivity (from about 6×10^{20} B cm⁻³ [18]). This increasing interaction introduces additional defects, which expands the lattice (see above) and decreases the growth rate [9]. They also average the growth rate between the various directions and therefore the selection described in the evolutionary model and the resulting fiber texture are lost.

5. Conclusion

The incorporation of boron in polycrystalline diamond films is shown to have a tremendous effect on both the diamond lattice parameter and the texture of the films.

The cubic lattice remains, but from 10^{17} to about 10^{19} B cm⁻³ the lattice parameter is smaller than that of undoped diamond. If we suppose that the defects are expanding the lattice, such a smaller value is ascribed to a decrease in the concentration of defects, from the effect of the doping level on the defect concentration, in agreement with our previous Raman measurements [9]. For B incorporation higher than 10^{19} cm⁻³, an impurity band is formed, with increasing interaction between B atoms resulting in the variation from hopping (starting at 10^{19} B cm⁻³) to metallic conduction at 6×10^{20} B cm⁻³ [18]. On the other hand, the B interaction introduces additional defects which expand the lattice, and progressively average the growth rate in all directions, resulting finally in the complete loss of the $\langle 111 \rangle$ texture when $[B] = 6 \times 10^{20}$ B cm⁻³.

Acknowledgement

The authors acknowledge DRET for partial financial support of this work.

References

- [1] S. Koizumi, T. Murakami, T. Inuzuka and K. Suzuki, *Appl. Phys. Lett.* 57 (1990) 563; D.N. Belton and S.J. Schmeig, *J. Appl. Phys.* 66 (1989) 4223.
- [2] J. Narayan, A.R. Srivatsa, M. Peters, S. Yokota and K.V. Ravi, *Appl. Phys. Lett.* 53 (1988) 1823; C. Wild, N. Herres, J. Wagner, P. Koidl and T.R. Anthony, *Electrochem. Soc. Proc.* 89 (1989) 283; K. Kobashi, K. Nishimura, K. Myata, K. Kumagai and A. Nakae, *J. Mater. Res.* 5 (1990) 2469; E.D. Specht, R.E. Clausing and L. Heatherly, *J. Mater. Res.* 5 (1990) 2351.
- [3] C. Wild, N. Herres and P. Koidl, *J. Appl. Phys.* 68 (1990) 973.
- [4] (a) R.E. Clausing, L. Heatherly, D. Specht and K.L. More, *New Diamond Science and Technology*, MRS Symp. Proc. (1991) p. 575; (b) Y. Tzeng, M. Yoshikawa, M. Murakawa and A. Feldman, *Applications of Diamond Films and Related Materials*, Eds. Y. Tzeng et al. (Elsevier, Amsterdam, 1991) p. 489; (c) C. Wild, R. Kohl, N. Herres, W. Muller-Sebert and P. Koidl, *Diamond and Related Mater.* 3 (1994) 373.
- [5] C. Wild, P. Koidl, N. Herres, W. Muller-Sebert and T. Eckermann, *Electrochem. Soc. Proc.* 91 (1991) 224.
- [6] B.R. Stoner and J.T. Glass, *Appl. Phys. Lett.* 60 (1992) 698.
- [7] X. Jiang and C.-P. Klages, *Diamond and Related Mater.* 2 (1993) 1112; X. Jiang, C.-P. Klages, R. Zachai, M. Hartweg and H.-J. Füsser, *Appl. Phys. Lett.* 62 (1993) 3438.
- [8] R. Khol, C. Wild, N. Herres, P. Koidl, B.R. Stoner and T. Glass, *Appl. Phys. Lett.* 63 (1993) 1792.
- [9] E. Gheeraert, P. Gonon, A. Deneuve, L. Abello and G. Lucazeau, *Diamond and Related Mater.* 2 (1993) 742.
- [10] L.G. Schulz, *J. Appl. Phys.* 20 (1949) 1030.
- [11] H.R. Wenk, *J. Appl. Cryst.* 25 (1992) 524.
- [12] D. Chateigner, P. Germi and M. Pernet, *J. Appl. Cryst.* 25 (1992) 766.
- [13] D. Chateigner, F. Brunet, P. Germi, M. Pernet, A. Deneuve and E. Gheeraert, to be published.
- [14] J.G. Ran, G.Q. Zheng, J. Ren and S.M. Hong, *Diamond and Related Mater.* 2 (1993) 793.
- [15] O.A. Voronov and A.V. Rakhmanina, *Inorg. Mater.* 29 (1993) 707.
- [16] B.V. Spitsyn, L.L. Bouilov and B.V. Derjaguin, *J. Crystal Growth* 52 (1981) 219.
- [17] A. van der Drift, *Philips Res. Rep.* 22 (1967) 267.
- [18] P. Gonon, A. Deneuve and E. Gheeraert, unpublished.